Catalog-based atmosphere uncertainty quantification

Alejandro Cano, Manuel Sanjurjo-Rivo, Joaquín Míguez
Universidad Carlos III de Madrid, Avenida Universidad 30, Leganés 28911, Spain
alejandro.cano@alumnos.uc3m.es, joaquin.miguez@uc3m.es, manuel.sanjurjo@uc3m.es
Alejandro Pastor, Diego Escobar
GMV, Calle Isaac Newton 11, Tres Cantos, 28670, Spain
apastor@gmv.com, descobar@gmv.com

ABSTRACT

Due to the ever-increasing space objects population, Space Situational Awareness (SSA) products and services have become the cornerstone for the safety and sustainability of spacecraft operations. Most of these services rely on the characterization of the uncertainty of the system, which is known as Uncertainty Quantification (UQ). In many applications the uncertainty of the orbit state is represented by the covariance matrix, obtained from an Orbit Determination (OD) process. However, typical OD processes, usually consider the measurements noise as the only source of uncertainty. An unrealistic characterisation of the uncertainty of dynamical and observation models leads to a degradation of the realism of the covariance, and jeopardizes spacecraft operations.

In this work, we apply our recent methodology for covariance realism improvement, based on the consider parameter theory of batch least-squares methods, to a catalog scenario to derive the uncertainty of the atmospheric drag model. This methodology infers the variance of consider parameters based on the observed distribution of the Mahalanobis distances of the orbital differences between predicted and estimated orbits, which theoretically should follow a chi-square distribution under Gaussian assumptions. Empirical Distribution Function (EDF) statistics such as the Cramer-von-Mises or the Kolmogorov-Smirnov distances are used to determine optimum variances of such parameters for covariance realism.

In Low Earth Orbit (LEO), the main source of uncertainty arises from the interaction of the atmosphere with the satellite motion, the atmospheric drag. The main objective of this work is to adapt and test the previously developed methodology to a LEO catalog scenario, in which the evolution of the density uncertainty for multiple objects can be analysed together by modelling such uncertainty as a consider parameter. Thus, instead of estimating consider parameter variances tailored to a single object during a long period, the objective of this work is to determine variances of parameters of an uncertainty model for the atmospheric density, improving the covariance realism for different clusters of cataloged objects (i.e. different altitudes or ballistic coefficient). Altitude-dependent models of the atmospheric density uncertainty, based on statistical analysis of historic space weather data, are applied for realistic simulations together with space-correlated density perturbations. Results are presented focusing on the physical interpretation of the determined consider parameter model variances and their effectiveness for improving the covariance realism of the considered catalog of objects.

1. INTRODUCTION

In the current over-populated space environment, the provision of Space Situational Awareness (SSA) and Space Traffic Management (STM) services and products is becoming the cornerstone for safe and efficient spacecraft operations. Many of these services, such as conjunction risk assessment, maneuver detection, fragmentation analysis or catalog build-up and maintenance require reliable estimations of the state of the Resident Space Objects (RSOs) and their associated uncertainty. The quality of this uncertainty is generally measured by how closely it represents reality, also known as uncertainty realism.

Under the assumption that the state of an orbiting object can be represented by Gaussian random variables, the Probability Distribution Function (PDF) of a state can be reduced to its two first statistical moments (i.e., mean and variance).

Despite of these strong assumptions, most operational scenarios represent the RSO state with its mean state and covariance matrix, the main outputs of typical Orbit Determination (OD) processes. Though the latter is only a necessary but not sufficient condition for uncertainty realism, in this framework uncertainty realism is reduced to covariance realism. This uncertainty representation avoids handling more complex PDF representations of the state, being a recurrent choice for SSA operational scenarios where data scarcity and the large number of objects have increased the complexity of the system. Nonetheless, covariance realism still requires an unbiased estimation and covariance consistency in terms of size, shape and orientation.

Typical OD processes, based on batch least-squares algorithms, normally consider the measurements noise as the only source of uncertainty [1], giving the covariance of the estimated state the name of noise-only covariance [2]. However, dynamic or measurement model uncertainty sources are typically disregarded. This leads to a lack of realism in such covariance matrices, being overly optimistic, thus jeopardizing SSA products reliability. This lack of covariance realism is caused by an improper characterization of some of the uncertainty sources present in the underlying models and parameters used to represent the orbital motion [3, 4].

Therefore, it is crucial for SSA activities and the future sustainability of the space environment to improve the modelling and characterisation of the RSO uncertainty, which is the goal of Uncertainty Quantification (UQ). Among the many aspects of UQ, this work focuses on the so-called inverse problem, this is, the characterisation of the discrepancies between observations of a system and the models used to represent it [5]. Consequently, effective UQ methods that improve the modelling of the uncertainty result in an enhancement of the uncertainty realism.

A widely explored option to characterise the inherent uncertainty of the space environment is the introduction of stochastic dynamic models or process noise, modelling the uncertainty of the system as Brownian motion, Ornstein-Uhlenbeck or Gauss-Markov processes [6, 7]. Process noise techniques, mainly used in filtering applications, also consist in adding certain noise terms to the system dynamics to account for unmodelled uncertainty sources. Their main drawback is the estimation of the noise to be introduced in the system. For these reasons, process noise estimation via calibration processes are required to maintain a physical interpretation of the uncertainty [8, 9]. For instance, in [10], a physically-based estimation of a process noise matrix that models the drag uncertainty is proposed and applied to a batch estimation. In [11, 12, 13], the concept of empirical covariance matrices is proposed. The goal is to include the residuals of the orbit determination process for the estimation of the covariance, adapting faster to noise time variations than process noise techniques. However, the physical interpretation of the uncertainty sources cannot be unveiled with this technique.

Another approach is the parameter uncertainty, which models the uncertainty of the system as uncertain parameters whose distribution impacts the state uncertainty evolution. Depending on the type and observability of the parameter, its impact on the system time-evolution can be included [5]. An example of uncertain parameters methods is the *consider parameters* theory. It consists in expanding the state space with additional parameters in the dynamic or measurements models. These parameters intend to represent specific and tailored sources of uncertainty, and are devised to follow a certain model with its corresponding uncertainty, in this case, a Gaussian distribution with null mean (to get an unbiased estimation) and certain variance. Even though it has been classically applied to batch estimation, this formulation can be also combined with filtering algorithms such as the Schmidt-Kalman filter [14, 15]. Due to the correlation between those parameters and the dynamics, the state uncertainty evolution is affected by the additional variance of the considered parameters, providing a physically-based and traceable source for the modelled uncertainty. However, the consider parameter theory suffers from the same drawback as process noise techniques: realistic noise values or variances of such parameters are not normally known. Overly optimistic, or oversized, variances may fail to model the uncertainty of parameters in the estimation and subsequent propagation of the covariance, not achieving covariance realism.

There are other techniques to improve the realism of the uncertainty of the state without focusing on the modelling and estimation of the different sources of uncertainty. The representation of the state in slowly-varying set of elements allows to maintain Gaussianity for longer propagation arcs and thus reduce the realism degradation, such as mean orbital elements [16, 17] or non-linear reference frames [18]. Covariance inflation techniques are also applied in many operation centres such as the Space Operations Center (CSpOC) [5], using scaling factors for the covariance to improve its realism. Some authors propose the use of such factors based on matching the initial position uncertainty with the velocity error [19]. Others explore the use of the Mahalanobis distance of the orbital differences to find global covariance scaling factors [20]. Even though these methods can be effective under some assumptions, they do not allow to study the physical meaning of the correction.

In previous works, we have developed a covariance determination methodology to improve covariance realism during orbit determination and propagation, based on the consider parameter theory, orbital differences between estimated and predicted orbits and the χ^2 distribution [21, 22, 23]. The core of the method is that, under Gaussian assumption, the difference between both orbits projected into the covariance space, i.e., Mahalanobis distance, must follow a χ^2 distribution. Thus, the variance of the consider parameters can be determined via statistical comparison between the observed Mahalanobis distance distribution and the expected one, i.e., a χ^2 distribution. This is, our methodology follows the uncertain parameter approach of UQ, modelling specific uncertainty sources with the *consider parameters* theory. If the variance of such parameters is properly inferred with the proposed methodology, the consider parameter theory correction acts as a covariance inflation technique. Thus, the covariance shape and scale are modified according to the physical sources of uncertainty that are included, hence improving the realism of the covariance. In previous works, the proposed methodology has been validated and tested in simulated scenarios for LEO [21] and GEO [22], with different sources of uncertainty analysed, as well as with real data [23]. However, previous studies were focused on a single RSO analysis, with an assumed constant variance of the consider parameter models.

In the present work, the goal is to apply the covariance determination methodology [21] in a LEO catalog-like scenario. In this orbit regime, the drag force becomes of high relevance for the orbit dynamics, turning into the dominant perturbation for low of altitudes. In addition, this force is subjected to several sources of uncertainty that are normally disregarded in nominal batch least-squares OD processes. Firstly, in SSA applications for non-collaborative objects, the drag coefficient, mass and area of the RSO is subject to a high level of uncertainty [2]. Secondly, the atmospheric density is also an uncertain parameter, both due to the lack of knowledge in the density models (presenting variations of even a 10-20% between them [24, 25]) and also due to its dependence on the solar activity prediction. For all these reasons, the evolution of the drag uncertainty and the atmospheric density as a function of the altitude, RSO characteristics or solar activity is subject to many studies [26, 24, 6, 7, 27, 28, 29]

Therefore, this work expands the previously developed methodology of [21] to estimate parameters that define the variation of the atmospheric density uncertainty in space environments. To this end, we apply a statistical analysis of historical space weather data to derive a parametric law for the evolution of the density uncertainty with altitude, for a given period of high solar activity, based on the work developed in [30, 31]. Using this law, a simulation with several objects at different altitudes is carried out, applying realistic and space-correlated perturbations derived from the uncertainty evolution law. Finally, the covariance determination methodology is applied simultaneously to all objects with the objective of estimating the parameters that define the evolution of the density uncertainty.

The remainder of the paper is structured as follows: Section 2 describes the methodology of the analysis. This includes a summary of the covariance determination methodology principles in Subsection 2.1, the development of the catalog-based adaptation and the historical statistical analysis for the atmospheric density standard deviation in Subsection 2.2, and finally a description of the simulation environment in Subsection 2.3. Next, Section 3 presents the results of the analysis. Finally, Section 4 summarizes the main conclusions and future work.

2. METHODOLOGY

This section describes the methodology of this work. First the main aspects of the covariance determination method are outlined. Then, the altitude-dependent model for the atmospheric density uncertainty is developed. Finally, the details of the simulation process are explained.

2.1 Covariance determination method principles

This section summarizes the background of the covariance determination methodology developed in [21].

2.1.1 Consider parameter theory

The covariance determination method is based on the *consider parameters* theory, whose complete description can be found in [1, 4]. Let us define first the estimated parameters vector used in a batch least-squares process as

$$\mathbf{y_{est}} = \begin{pmatrix} \mathbf{r}(t_0) \\ \mathbf{v}(t_0) \\ \mathbf{p}(t_0) \end{pmatrix} \in \mathbb{R}^{n_y} \tag{1}$$

being $\mathbf{r}(t)$, $\mathbf{v}(t)$ and n_y the position, velocity and estimated state dimension, respectively. $\mathbf{p}(t)$ represents the vector of dynamical parameters, either applied to the force or the measurement models. A common dynamical parameter in LEO is the drag coefficient (C_d). Let us represent the considered parameters that are modelled in the system in a consider parameter vector as

$$\mathbf{y}_c = \begin{pmatrix} c_1 \\ \vdots \\ c_{n_c} \end{pmatrix} \in \mathbb{R}^{n_c} \tag{2}$$

where n_c is the number of consider parameters. They are defined to follow a Normal distribution of the form

$$c_i \sim \mathrm{N}\left(0, \sigma_i^2\right) \quad \text{with} \quad i = 1, \cdots, n_c \tag{3}$$

The *consider parameters* theory models the parameters with zero mean to keep the expected value of the estimation unbiased [4]. On the contrary, the covariance of the estimation is affected by the consider parameters. The consider covariance is then

$$\mathbf{P}_c = \mathbf{P}_n + \left(\mathbf{P}_n \mathbf{H}_y^T \mathbf{W}\right)\left(\mathbf{H}_c \mathbf{C} \mathbf{H}_c^T\right)\left(\mathbf{P}_n \mathbf{H}_y^T \mathbf{W}\right)^T \tag{4}$$

where $\mathbf{H_y}$ and $\mathbf{H}_c$ correspond to the Jacobian of the observations with respect to the estimated parameters and consider parameters, respectively. $\mathbf{W}$ represents the weighting matrix containing the expected noise of each measurement and the possible correlation among them. $\mathbf{P}_n$ is the so-called noise-only covariance, this is, the nominal estimation output of a batch least-squares estimation, inverse of the normal equations matrix, i.e.,

$$\mathbf{P}_n = \left(\mathbf{H}_y^T \mathbf{W} \mathbf{H}_y\right)^{-1} \in \mathbb{R}^{n_y \times n_y}. \tag{5}$$

Finally, $\mathbf{C}$ is defined as

$$\mathbf{C} = \begin{pmatrix} \sigma_1^2 & \cdots & 0 \\ \vdots & \ddots & \vdots \\ 0 & \cdots & \sigma_n^2 \end{pmatrix}, \tag{6}$$

containing the variances of the consider parameters, where no correlation between them is assumed. Eq. (4) can be written as

$$\mathbf{P}_c = \mathbf{P}_n + \mathbf{K}\mathbf{C}\mathbf{K}^T \in \mathbb{R}^{n_y \times n_y}, \tag{7}$$

with

$$\mathbf{K} = \mathbf{P}_n \left(\mathbf{H}_y^T \mathbf{W} \mathbf{H}_c\right) \in \mathbb{R}^{n_y \times n_c} \tag{8}$$

Therefore, the consider covariance is obtained as the noise-only covariance plus a covariance correction, which depends linearly on the consider parameter variances. The objective of the covariance determination methodology is to find the variances of the consider parameters such that realistic covariance estimations are obtained.

We restrict our analysis to linear regimes and Gaussianity assumption. For these reasons, more complex and accurate uncertainty propagation methods are out of the scope of this work. Additionally, linear propagation methods are common in many SSA scenarios due to its reduced complexity, lower computational cost, and suitability for relatively short propagation intervals. The consider covariance can be linearly propagated as

$$\mathbf{P}_c(t) = \Psi(t, t_0)\, \mathbf{P}_c(t_0)\, \Psi(t, t_0)^T \tag{9}$$

where $\Psi(t, t_0)$ is the extended transition matrix, which connects the position and velocity at any time t with respect to the initial state and dynamic parameters at time t_0. It contains the state transition and sensitivity matrices, and

can be computed via numerical integration of the variational equations of motion of the system [4]. The length of the propagation arcs where such linear and Gaussian assumptions hold can vary significantly depending on the RSO characteristics or altitude. To assess whether such assumptions are valid during the simulations, Gaussianity tests are applied. Michael's normality test has been chosen for the work presented here [32, 33].

2.1.2 Considered parameters variance estimation

To determine the unknown variance of the consider parameters that improve the consider covariance realism, we resort to the properties of the Mahalanobis distance and the χ^2 distribution under Gaussian assumptions. The Mahalanobis distance (d_M) is a well-known statistical metric that describes how far a state $\mathbf{y}(t)$ is from a certain reference $\mathbf{y}_{ref}(t)$, projected into the covariance space [34]. The squared Mahalanobis distance is defined as

$$d_M^2 = \left(\mathbf{y}-\mathbf{y}_{ref}\right)^T \left(\mathbf{P}+\mathbf{P}_{ref}\right)^{-1} \left(\mathbf{y}-\mathbf{y}_{ref}\right) \tag{10}$$

where $\mathbf{P}$ and $\mathbf{P}_{ref}$ are the covariance matrices of the state and the reference, respectively. Both matrices are computed using Equation 9, from different estimation processes. In Eq. 10, it is assumed that both variables $\mathbf{y}$ and $\mathbf{y}_{ref}$ are uncorrelated. This same assumption, applied in other studies such as in [5] or [35], is not easily guaranteed in many scenarios, for instance, when the same sensor network is shared for both estimations. In the case of the covariance determination process described here and in [21], such correlation is mitigated by ensuring that the computed reference orbit does not share any observation with the orbit state under analysis as further explained in [21]. Combining Eq. 7 with Eq. 10, the squared Mahalanobis distance can be expressed as

$$d_M^2(t) = \Delta\mathbf{y}(t)^T \left(\Psi\left(t,t_0\right)\left(\mathbf{P}_n+\mathbf{K}\mathbf{C}\mathbf{K}^T\right)\Psi\left(t,t_0\right)^T+\mathbf{P}_{ref}(t)\right)^{-1} \Delta\mathbf{y}(t) \tag{11}$$

where $\Delta\mathbf{y}(t) = \mathbf{y}(t)-\mathbf{y}_{ref}(t)$. Therefore, Eq. 11 allows to compute the Mahalanobis distance at any epoch along the propagation arc as a function of the consider parameter variances, present in matrix $\mathbf{C}$.

Bearing this in mind, the covariance determination concept is as follows. Firstly, the χ^2 distribution is defined as the sum of squared Normal distributions [36]. In that case, if the Mahalanobis distance between the state and its reference is computed with a well-characterised covariance (i.e. realistic), the squared Mahalanobis distance should follow χ^2 distribution under Gaussian assumptions. Therefore, it is possible to use Eq. 11 to determine the variance of the considered parameters such that the observed squared Mahalanobis distance distribution resembles the expected theoretical behaviour of the χ^2 one. This is done by the minimisation of an Empirical Distribution Function (EDF) metric, which can be used to determine the resemblance between two Cumulative Distribution Function (CDF). Among the multiple options available in the state-of-the-art [36, 5], two well-known EDF metrics have been chosen and tested in [21], the Kolmogorov-Smirnov and Cramer-von-Mises metrics.

Finally, it is necessary to define which orbit is to be used as reference for the Mahalanobis distance computation of Eq. 11. As described in [21], the propagation arc of each orbit is compared against the estimation arc of a newer orbit, since the error of propagating a certain estimation is expected to be larger than the estimation error, bounded by observations. To summarize, the covariance determination methodology proposed in [21] consists in, given a population of orbits, find the variance of the consider parameters that lead to consider covariance matrices that are representative of the dispersion observed in the orbital differences, by means of the minimisation of an EDF metric.

2.2 Catalog atmospheric density uncertainty

The objective of this work is to apply the covariance determination methodology to estimate not only the uncertainty of a singular RSO, but to estimate the evolution of the atmospheric model uncertainty as a function of the altitude in a catalog. This section describes the rationale behind the input uncertainty in the simulations carried out and how this uncertainty is estimated for a catalog of objects.

2.2.1 Space weather statistical analysis

To test the performance of the methodology, a representative atmospheric density uncertainty as a function of altitude has been used. The applied atmospheric density uncertainty model is based on the work carried out in [30] and [31].

In these works, the uncertainty of the atmospheric density is assessed by analysing the effect of the solar proxies dispersion in the density output of the NRLMSISE00 model. Historical space weather proxies from 1957 up to 2020 (from Celestrak [37]) are processed to select different solar activity strata (in terms of F10.7 solar flux) and identify epochs of reference for each stratum with moving-averaged proxies, as can be seen in Fig. 1

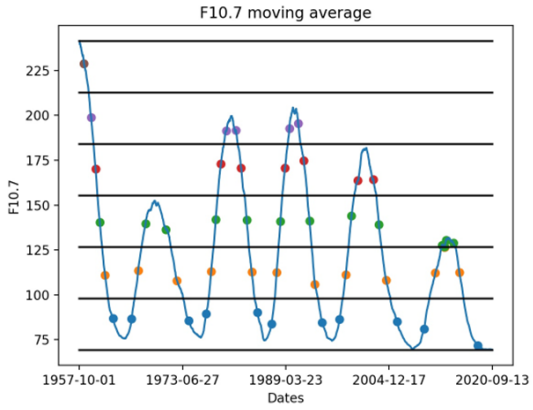

Fig. 1: Example of 6 different solar activity strata and their reference epochs, from [31].

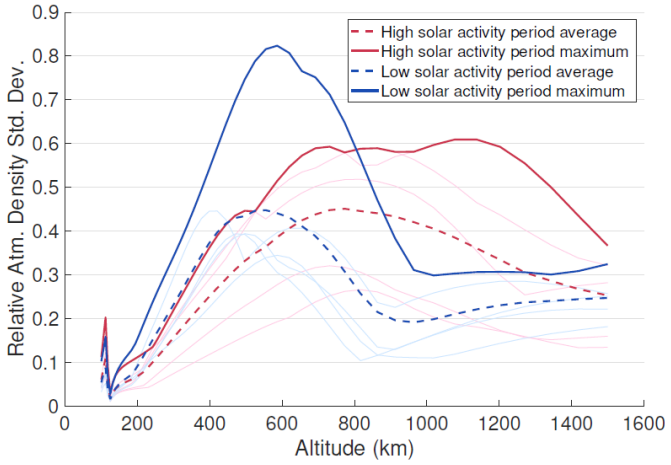

Fig. 2: Averaged and maximum uncertainty curves for periods of high and low solar activity (solid lines) and original ones for each period of both strata (glassy lines), from [30].

Next, at each reference epoch and solar activity strata (each point of Fig. 1), an artificial joint random distributions is built, considering the correlation between geomagnetic and solar activity in the surrounding months of the reference epochs. In parallel, a 3-dimensional grid of latitude, longitude and altitude is constructed. Then, 1000 samples of each joint distribution (i.e. one per point in Fig. 1) are drawn and provided as input to the NRLMSISE00 model at each point of the 3-dimensional grid. The atmospheric density outputs are aggregated, and a standard deviation is obtained for each node, solar activity stratum and reference date. Finally, the maximum standard deviation for each altitude and solar activity is stored, retaining as a conservative measure the maximum standard deviation in the latitude/longitude grid of each altitude.

Fig. 2, from [30], depicts the evolution of relative density standard deviation with altitude, in a two-strata analysis of low or high solar activity. The glassy lines correspond to the uncertainty curves at different reference epochs, for both activity levels. The solid lines correspond to the maximum uncertainty values between all reference dates, whereas dashed lines represent the average value. The relative standard deviation of the density is larger for low solar activity periods. In both periods of low and high solar activity levels, the standard deviation shows a linear growth between approximately 300 km and 500 km, followed by growth rate decrease around 600 km for low activity, and 700 km for high activity. In the work presented here, the high solar activity average standard deviation curve (dashed red line of Fig. 2) has been chosen to represent the evolution of the density standard deviation in the simulations.

2.2.2 Altitude parametrization

Once it has been explained how a statistically representative evolution of the density standard deviation with altitude has been chosen, this subsection describes how the model of atmospheric drag uncertainty is parametrized and how the covariance determination methodology is adapted to estimate the evolution of the uncertainty with altitude.

First of all, it is necessary to define the consider parameter model for the atmospheric drag. The classical drag acceleration equation including the aerodynamic model consider parameter is defined as:

$$\mathbf{a}_{\text{drag}} = -\frac{1}{2}\rho\frac{C_d A}{m}|\mathbf{v}_{\text{rel}}|^2\frac{\mathbf{v}_{\text{rel}}}{|\mathbf{v}_{\text{rel}}|}(1+c_{AE}), \tag{12}$$

where ρ is the atmospheric density, A the cross-sectional area, m the object mass, C_d the drag coefficient and $\mathbf{v}_{rel}$ is

the relative speed vector of the object with respect to the atmosphere. Finally c_{AE} is the consider parameter, defined to follow Eq. 3 as

$$c_{AE} \sim \mathrm{N}\left(0, \sigma_{AE}^2\right) \tag{13}$$

Its objective is to model the error in the atmospheric density and ballistic coefficient, this is, containing C_d, mass and cross-sectional area uncertainty. Since this work is focused on the uncertainty arising from the atmospheric density, mass and cross-sectional areas are assumed to be fixed and known quantities.

Now, the objective is to characterize the altitude evolution of the atmospheric density standard deviation by means of the consider parameter variance. To this end, the consider parameter standard deviation is parametrized as follows

$$\sigma_{atm}(h) = \sigma_{AE}(h,a,b,c) = a + bh + ch^2, \tag{14}$$

where h is the altitude. A second-order polynomial has been chosen among other families of fitting functions or polynomials based on a trade-off between accuracy and simplicity. Fig. 3 depicts the dataset for the density standard deviation curve in the averaged high solar activity (dashed red line of Fig. 2), with a numerical fit to the polynomial of Eq. 14. The Root Mean Square (RMS) error of the fitting suggests that the polynomial used is satisfactory. The results of this fitting are used as reference values in the simulated scenario, namely: $a_{tg} = -3.72 \cdot 10^{-1}$, $b_{tg} = 2.06 \cdot 10^{-3}$, $c_{tg} = -1.29 \cdot 10^{-6}$,

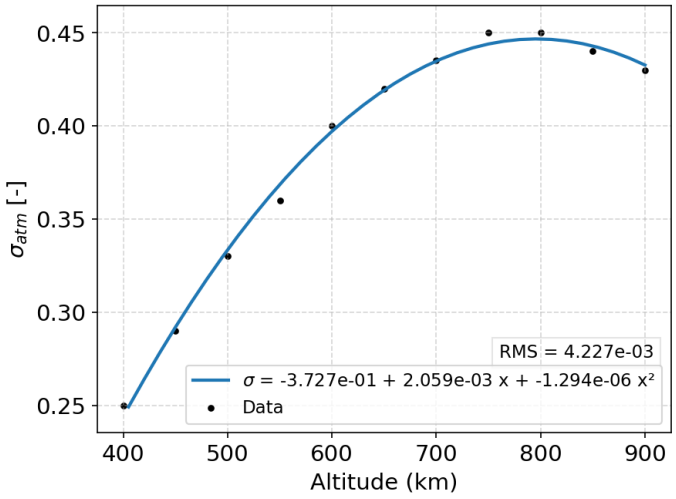

Fig. 3: Atmospheric density standard deviation data set and second-orbder polynomial fit

By combining the model of Eq. 14 with Eq. 11 for a single consider parameter, the Mahalanobis distance is obtained as a function of the parameters of the model (a,b,c). Thus, the problem at hand consists in the estimation of the parameters (a,b,c) that define $\sigma_{AE}(h,a,b,c)$ in the catalog scenario. In other words, the objective is to determine the parameters of the atmospheric density uncertainty model so that, at all altitudes, the population of Mahalanobis distances follow a χ^2 distribution, increasing the realism of all covariance matrices. To validate the performance of the covariance determination method to estimate such parameters, the results obtained with the fit of Fig. 3 are used as target values, as explained further in Section 2.3.3.

2.3 Simulation environment

Previous sections have described the evolution of the standard deviation of the atmospheric density, based on statistical analysis of historic space weather data. The ability and performance of the covariance determination methodology to characterise such density uncertainty model is assessed via simulations, whose details are explained in this section. The goal here is to maintain a simulation environment as realistic as possible, compatible with the described hypothesis and models, and representative of the current state of the LEO environment.

2.3.1 Simulation scheme

As discussed in Section 2.1.2, the proposed covariance determination methodology requires a population of Mahalanobis distances in order to estimate the variance of the consider parameters. Each Mahalanobis distance sample (Eq. 11) is retrieved from an orbit determination and propagation process. During the OD process, the noise-only covariance of the estimation is computed along with all components of matrix $\mathbf{K}$, which allows to compute the consider covariance at estimation epoch. However, the Mahalanobis distance must be evaluated at a propagation epoch so that the impact of errors in the atmospheric density can be observed as state vector differences. For this reason, the estimated state is propagated forward in time, obtaining in the process matrix Ψ to propagate the covariance linearly. The simulation scheme is as follows, analogous to all RSOs. More detailed information about this process can be found in [21]:

1. **Reference orbit**: a initial state is propagated forward in time with the dynamic model of Table 1. The length of the propagation will be determined by the amount of simulated data desired for the analysis. Previous studies of the covariance determination methodology have shown that an accuracy of 15% can be maintained with approximately 300 samples of a single object [21, 23]. Thus, the reference propagation has been set to obtain 300 ODs. This propagation does not contain any model error in the atmospheric density.
2. **Monte Carlo iterations**: the following sequence of steps is repeated in a similar fashion to a Monte Carlo scheme. Between each iteration, the reference state (taken from the *Reference orbit*), is shifted forward. Also, each iteration will use different density and measurements perturbations, as further described in Section 2.3.3.
   (a) **Perturbed orbit**: the reference state is propagated backwards 7 days in time, a common length for LEO OD arcs. During this propagation with the dynamic model of Table 1, a sample error of the atmospheric density is introduced, as described further in Section 2.3.3. This perturbation is applied as constant for the orbit time-span, as defined in the *consider parameters* theory.
   (b) **Measurements generation**: from that perturbed orbit, measurements are generated from ground-based radars with typical SSA radar noise (Table 2). During this process, real observability conditions are considered.
   (c) **Orbit determination**: with the synthetic measurements, an OD is performed in a 7 days arc. The estimation epoch (t_0) is automatically set to the epoch of the last observation.
   (d) **Orbit propagation**: the estimated state is propagated forward 10 days.

As it has been mentioned in Section 2.1.2, Eq. 11 requires an orbit to be used as reference. In this work, as concluded previously in [21], the applied estimated reference orbit consists in taking as reference, for orbit i under analysis, the orbit estimated in the Monte Carlo iteration $i+7$. The main reasons are two: firstly, in an operational environment, precise orbits are generally not available, specially for non-collaborative objects such as space debris; secondly, the error within the OD arc is expected to be bounded by the observations, and lower than the error during prediction (propagation). In order to reduce correlation between them, the orbit under analysis and the estimated reference orbit do not share any measurement. Note that the covariance of the latter orbit ($\mathbf{P}_{ref}$ in Eq. 11) is also affected by model errors, and thus the consider parameter correction is also applied to it.

2.3.2 Simulation setup

This subsection gathers the main characteristics of the simulation scenario. The details of the dynamic model applied for the high-fidelity numerical propagation are included in Table 1. The measurement Gaussian noise applied during the simulation of measurements is described in Table 2. Finally, the characteristic of the simulated radars are shown in Table 3.

2.3.3 Altitude correlated noise

On the one hand, we are modelling the atmospheric drag density error according to Eq. 13, each orbit determination and propagation affected by a sample of such distribution, acting as a constant perturbation. On the other hand, the

Table 1: Dynamical model

Reference frame	J2000 ECI
Gravity field	16x16
Third body perturbations	Sun & Moon
Polar motion and UT1	IERS C04 08
Earth pole model	IERS 2010 conventions
Earth precession/ nutation	IERS 2010 conventions
Atmospheric density model	NLRMSISE-00
Solar radiation pressure model	Cannonball
Drag model	Cannonball
Solar radiation pressure area	Constant area
Drag area	Constant area

Table 2: Measurement noise

Measurement type	σ	**Units**
Two-way range	10	m
Two-way range rate	300	mm/s
Azimuth and elevation	1	deg

Table 3: Characteristics of simulated radars

Field of view		Pyramidal asymmetric
Line of sight (southwards pointing)	**Azimuth**	180 deg
	Elevation	75 deg
Aperture	**Azimuth**	$\pm$43 deg
	Elevation	+15º/-10 deg
Geodetic coordinates radar 1 (Spain)	**Longitude**	-5.5911 deg
	Latitude	37.16643 deg
	Height	0.1423 km
Geodetic coordinates radar 2 (Germany)	**Longitude**	7.12961 deg
	Latitude	50.61657 deg
	Height	0.2929 km
Observation spacing		5 seconds

modelled atmospheric density uncertainty evolves solely as a function of altitude for a certain level of solar activity, according to the chosen model for the space environment. Since, under such hypothesis, two objects at the same altitude and time-frame should be affected by the same error in the density model, it would be physically incoherent to apply a completely different perturbation to objects at the same or nearby altitude at the same interval of analysis. Consequently, an altitude-correlated noise sequence is applied.

To achieve a zero-mean correlated noise sequence for the density error, an auto-regressive function with space correlation of order 1 has been applied in the simulations [38]. This is described next. First, let us assume that the correlation of two perturbations at two consecutive altitudes $z(h_n)$ and $z(h_{n-1})$, in discrete form, is as

$$r_z(h_n, h_{n-1}) = \mathrm{E}[z(h_n)\, z(h_{n-1})] = r_0(h_n)\, e^{-\alpha |h_n - h_{n-1}|}, \tag{15}$$

where $r_0(h_n) = \mathrm{E}\left[z(h_n)^2\right]$ is the power of the non-stationary perturbation. In this case, we want the power of the noise to coincide with the atmospheric density variance deviation at each altitude, this is,

$$r_0(h_n) = \sigma^2_{atm}(h_n) = (a_{tg} + b_{tg} h_n + c_{tg} h_n^2)^2. \tag{16}$$

The spatial correlation of Eq. 15 can be guaranteed with the auto-regressive model of order 1, AR(1), as

$$z(h_n) = a(n) z(h_{n-1}) + u(n), \tag{17}$$

with

$$a(n) = \frac{r_0(h_n)}{r_0(h_{n-1})} e^{-\alpha (h_n - h_{n-1})}, \tag{18}$$

$$u(n) \sim \mathrm{N}\left(0, \sigma_u^2(n)\right) \text{ and } \sigma_u^2(n) = r_0(h_n) \left[1 - \frac{r_0(h_n)}{r_0(h_{n-1})} e^{-2\alpha (h_n - h_{n-1})}\right], \tag{19}$$

where $\alpha = 1/h_\alpha$ $[1/km]$ represents the inverse of the altitude scale of correlation, which determines the strength of the correlation (h_α). $u(n)$ is the Gaussian component of the noise, with variance $\sigma_u^2(n)$, that also depends on the power noise and is inversely proportional to the correlation. With this noise model, the perturbation at each altitude is correlated with the noise at the previous altitude by means of the factor $a(n)$, governed by the correlation scale α. The stronger the correlation (i.e., the smaller α), the smaller the Gaussian component $u(n)$ in the noise sequence. The choice of α and its estimation is a planned future line of research. However, in the work presented here, the value of $h_\alpha = 300[km]$ was selected, to have a scale of correlation of approximately $1/3$ of the altitude span covered in the simulation. In order to generate the input sequence of noise, the parameters obtained from the fit to the statistical data in Fig. 3 are used to define $r_0(h_n)$, as indicated in Eq. 16.

Fig. 4 shows the correlated density perturbation sequence (in relative terms) for ten different OD arcs. It can be noted how the perturbations at consequent altitudes show a certain level of correlation, despite maintaining a Gaussian component. Fig. 4 shows only ten OD arcs, for visualization purposes. If all perturbations at the same altitude and all OD arcs were analysed, those perturbations would follow a Normal distribution with a standard deviation from Eq. 16, maintaining the proper uncertainty input for the simulations.

2.3.4 RSO population

In this subsection, a brief description of the objects that have been used in the simulations is provided. The goal is to represent the LEO population for the catalog analysis under the previously described methodology. Recalling the definition of the consider parameter variance as a function of altitude (Eq. 14), objects at the same epoch and similar altitudes would suffer the same atmospheric density error. Therefore, under such model, it is only necessary to include an RSO per altitude in the catalog simulation, since according to such (strong) assumption, the uncertainty estimated would be representative for all objects at that altitude. The process to generate the RSO population has been the following:

1. Starting from SpaceTrak TLE LEO catalog [39], we retain objects of nearly-circular orbits and whose altitude is between 400 and 900 km.
2. Each objects is provided with a ballistic coefficient randomly selected from a distribution of typical values in the LEO catalog
3. An altitude grid of 15 km width, from 400 km up to 900 km is built. A single object inside each altitude grid is stored, filtering for Ballistic coefficients in the range 10-40.

Fig. 5 depicts the RSO population meeting conditions 1 and 2 of the above list (blue dots), and the finally chosen RSOs (red dots), with a total of 35 randomly selected objects.

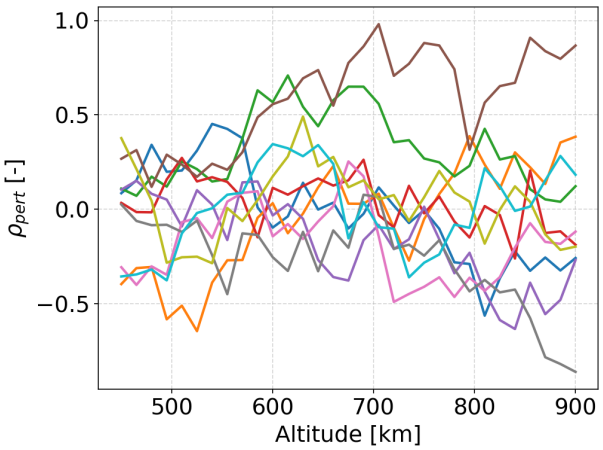

Fig. 4: Relative density perturbation as a function of altitude for 10 different OD arcs

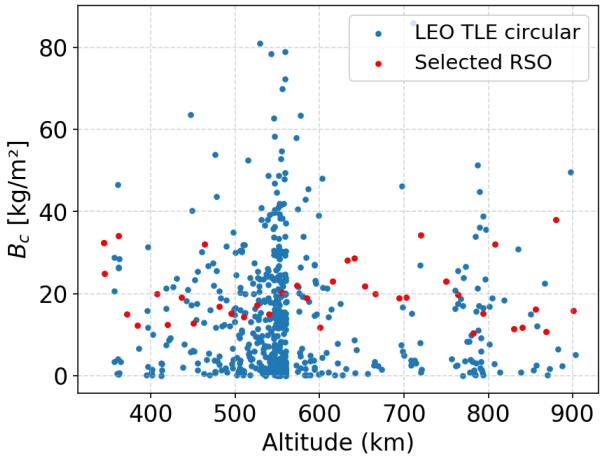

Fig. 5: All RSOs in circular LEO orbits with assigned ballistic coefficients (blue dot) and the selected RSOs for the analysis (red dots)

3. RESULTS

This sections presents and discusses the results of the catalog-based covariance determination in the described simulated scenario. Before presenting the final results, there are some intermediate Gaussianity analysis worth mentioning. If the orbital differences are not normally distributed, the uncertainty of the system cannot be represented by a covariance matrix. In this simulated scenario, where objects have different ballistic coefficients and altitudes, the time of validity for the linearity and Gaussian assumptions varies significantly, for instance, between altitudes lower than 500 km and those above 800 km. To mitigate this problem, the epochs of analysis for the orbital differences have been set between $t_0 + 1$ and $t_0 + 3$ days (where t_0 refers to the estimation epoch).

In addition to this, Michael's normality tests, were applied to the orbital differences of each object. It is one of the most suited tests for orbital differences analysis due to its powerful tail outlier rejection capabilities [40]. It provides a visual representation of the acceptable Gaussianity region in a percentile plot, and points laying outside can be visually identified. Fig. 6 show the Michael's test results separating the orbital differences components in RIC local frame (radial, in-track, cross-track [2]), but aggregating all objects and epochs of analysis. It is seen that many points lay outside the normality region in the radial and cross-track directions. On the contrary, normality is preserved on the in-track direction, as seen in Fig. 6c. Upon these results, the radial and cross-track directions were discarded from the computations of the Mahalanobis distance, shifting from a 3 DOF to a 1 DOF expected χ^2 distribution. Despite maintaining only the in-track component, this direction should be enable to capture atmospheric density errors, since the in-track direction is aligned with the velocity vector, direction in which the atmospheric drag acts on the objects.

The final results are gathered in Fig. 7, which compares the statistical curve of the atmospheric density uncertainty (blue line) with the curve estimated using the catalog-based covariance determination method (orange line). Fig. 7 also contains the input noise reconstruction curve at each altitude (green points), as well as it's second-order polynomial fit (dashed green line). The individual consider parameter standard deviations obtained by analysing each object individually are represented as orange dots. The estimated coefficients of the parametric function can be found in Table 4, comparing the results with the second-order fits to the model and input reconstruction. In addition, the RMS of the differences between the estimated curve and both the model and the input reconstruction is also showed.

It can be noted in Fig. 7 that the input reconstruction does not follow exactly the statistical model for the density standard deviation. The reason is the amount of samples (orbits) used per altitude grid, in this case, 300. This choice was a trade-off between data quantity and accuracy. The green curve converges to the blue one with increasing the amount of samples. The individual results of each object are shown for reference. It is seen that the uncertainty recovered for the objects individually is subject to a certain error, as was expected due to the 300 samples choice. Regarding the estimated parameters with the covariance determination methodology, the difference with respect to the

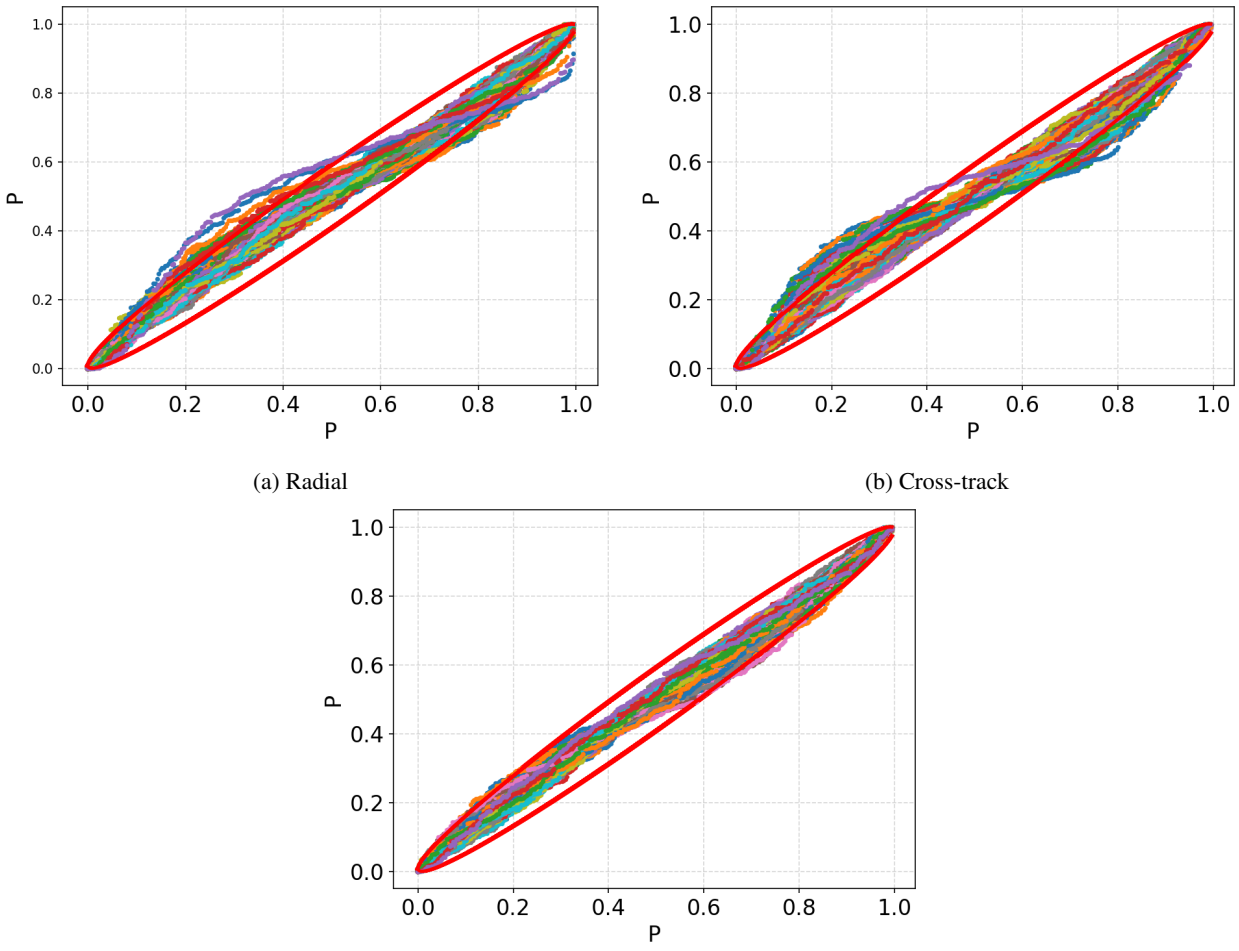

(a) Radial

(b) Cross-track

(c) In-track

Fig. 6: Michael's test results for in-track orbital differences for all objects and analysis epochs

density uncertainty model varies between 40% and 20%, as shown in Table 4. Even though this difference appears to be significant, the resulting curve of atmospheric density standard deviation with altitude is similar to the model one, as can be seen by comparing both curves in Fig. 7 and in the RMS value of 0.0096 of Table 4.

Moreover, regarding the differences between the estimated parameters and the resulting ones from a second-order fitting to the reconstructed input in Table 4, the accuracy of the method in this case is improved up to a range of 23%-14% in terms of parameters, and an RMS of 0.0086. This indicates the performance of the methodology to characterise the input uncertainty, even though this latter does not follow precisely the chosen model due to the samples limitation. However, in both cases, the RMS results of comparing the models in Table 4 correspond to than 2.2% of the maximum standard deviation, indicating a satisfactory accuracy in terms of atmospheric density standard deviation. It is seen how, when estimating the uncertainty evolution parameters using all the data from the selected catalog, the resulting curve is similar to a best-fit for the individual objects results, allowing a mitigation of individual errors and outliers of the objects in the catalog.

Fig. 8 shows the final distribution of the squared Mahalanobis distance samples, coming from all orbits of all objects in the considered catalog, when applying the estimated constants of the consider parameter variance. As discussed previously, only 1 DOF is considered in the optimisation, the in-track component. A satisfactory match between the squared Mahalanobis distance CDF and PDF and the χ^2 distribution can be appreciated in Fig. 8, confirmed with the metric of the fitting process, where Cramer-von-Mises test statistic was used. A metric of 0.19 is obtained, shown at the header of Fig 8, whereas the upper limit for the Cramer-von-Mises test statistic to reject the null hypothesis

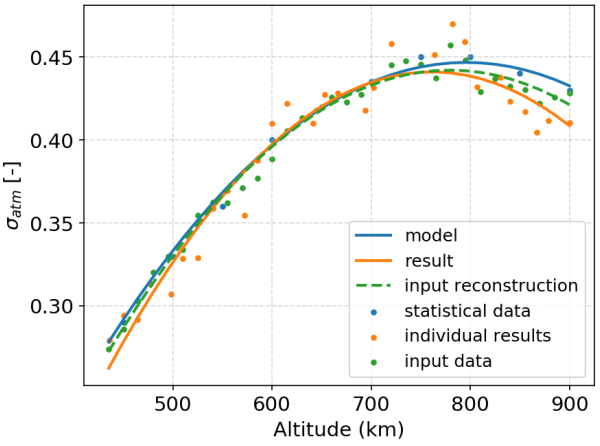

Fig. 7: σ_{AE} evolution results

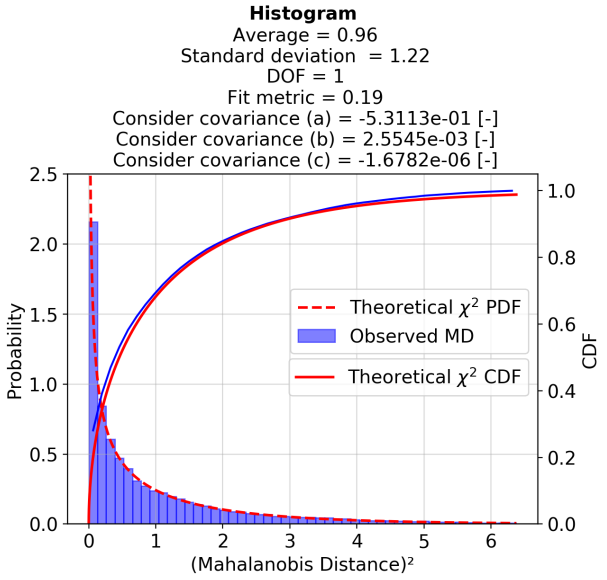

Fig. 8: Optimized squared Mahalanobis distance distribution for all objects. 1 Degree of Freedom (in-track), analysis window between t_0+1-t_0+3

Table 4: Results of the atmospheric density standard deviation parameters

	a [-]	b [-]	c [-]	RMS [-]
Estimated	$-5.31\cdot10^{-1}$	$2.55\cdot10^{-3}$	$-1.68\cdot10^{-6}$	-
Input reconstruction	$-4.29\cdot10^{-1}$	$2.24\cdot10^{-3}$	$-1.43\cdot10^{-6}$	-
Model	$-3.72\cdot10^{-1}$	$2.06\cdot10^{-3}$	$-1.29\cdot10^{-6}$	-
Difference w.r.t input [%]	23.90	13.84	17.5	0.0080
Difference w.r.t model [%]	42.74	23.78	30.23	0.0096

is 1.167. Thus, the test determines that the observed distribution, after the consider parameter correction, provides a strong match with the χ^2 distribution, in this case with a significance level of 0.25.

It is important to remark that all samples, coming from orbital differences of distinct objects and orbits, can be treated as part of the same distribution thanks to the Mahalanobis distance. When affected by the same perturbation in density, the error in position will depend significantly on the object altitude, position, ballistic coefficient. Nonetheless, the evolution of the covariance is also proportional to those factors. This normalization of the errors allows all Mahalanobis distances to belong to the same distribution, provided that the model errors are properly characterized and under certain assumptions such as Gaussianity and linearity, as previously discussed. Analogously, the covariance will also adapt for different orbit visibility and geometry factors that impact the OD process.

The results of the Cramer-von-Mises test is a marker of the covariance realism improvement that is obtained with the covariance determination methodology in the considered catalog of objects. However, this realism improvement is only ensured in the in-track direction. Even though this component of the state vector in local reference is the most affected by atmospheric density errors, it is necessary to assess the improvement in realism in all position components. For this purpose, covariance containment tests, as proposed in [41], allow for a clear physical insight and visual representation of the level of realism of the covariance. To evaluate if the covariance is representative of the orbital differences, the Mahalanobis distance can be used as a metric to see the amount of points that lay inside a $k\sigma$ ellipsoid ($k=1,2,3,4$) and compare it against the expected fraction for a multivariate Gaussian distribution of the same number of DOF. In this case, the interest lay in assessing the containment in full position (i.e., 3 DOF) that is achieved with the parameters that were estimated with the catalog-based covariance determination. Figures 9a and 9b show the visual representation of the containment test for two different objects in the analysed catalog, for a 3σ containment.

Each of the points correspond to orbital differences between estimated and predicted orbits, for different ODs. Fig. 9a corresponds to an object at a high altitude (830 km), showing a 3σ containment of 96.59%. Such containment is similar to the 97.1% value of 3σ theoretical containment for a 3 DOF multivariate Gaussian distribution. The samples of orbital differences are less dispersed in the in-track direction as compared to Fig. 9b. The latter corresponds to the object in a worst case scenario, this is, at low altitude (477 km) with a low ballistic coefficient, showing a 3σ containment of 92.03%. In fact, non-linearity is building up in 9b, where the so-called banana-shape of the orbital differences start to appear. As a consequence, the containment in 9b is lower than in its counterpart of 9a. Consequently, extreme care must be taken in terms of linearity and Gaussian assumptions when a catalog of objects is analysed.

Table 5 presents the average containment tests results for the complete catalog in two different cases: with the noise-only covariance (i.e. without any model error correction) and with the consider covariance (i.e. the resulting covariance when applying the consider parameter variance obtained with the covariance determination process). An average containment similar to their expected fractions at the different $k\sigma$ levels is seen, what indicates an overall covariance realism improvement for the catalog as compared to the containment obtained with the noise-only covariance, which fails to model the uncertainty of the system in the present of dynamic model errors. In fact, the similarity between the containment tests and the theoretical expectations at all σ level indicates that the covariance determination methodology does not oversize the covariance matrices.

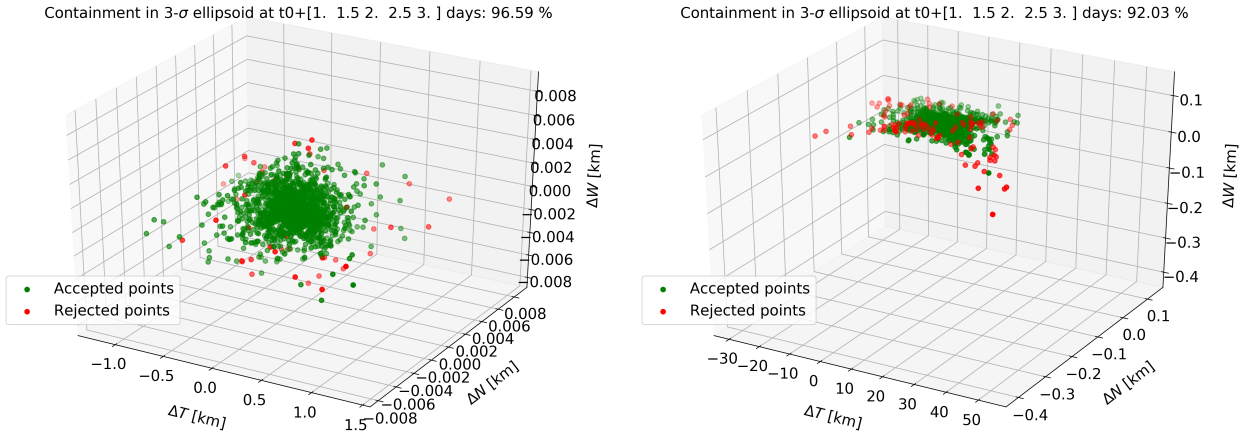

(a) Object # 6, at 830 km altitude

(b) Object # 27, at 477 km altitude

Fig. 9: Covariance containment test at 3σ level for 3 DOF, using the optimum estimated parameters results. Theoretical 3σ containment for a multivariate Guassian distribution of 3 DOF is 97.1% [41]

Table 5: Average covariance containment tests (in %) for selected catalog of objects.

	1σ	2σ	3σ	4σ
Noise-only covariance	0.25	1.40	2.87	4.37
Consider covariance	19.20	72.93	96.64	99.80
Theory (3DOF)	19.90	73.90	97.10	99.87

4. CONCLUSIONS AND FUTURE WORK

The goal of the presented work was to extend the covariance determination methodology to a catalog scenario, in which the evolution with altitude of the atmospheric density uncertainty could be estimated. To this end, a parametric, altitude-dependent function of the density standard deviation has been applied as consider parameter model, switching the covariance determination process to the estimation of the parameters that define such model by considering a catalog of objects. In line with the statistical analysis of historic space weather data and its impact on density estimation, a second-order polynomial was chosen to model the evolution of relative density standard deviation with altitude, and the resulting uncertainty curve for a high solar activity period was used as reference model for the simulations. The validation of the methodology was carried out in a simulated environment, having several orbit determination and propagation steps for each object in the chosen catalog, adding space-correlated perturbations to the atmospheric density according to the reference second-order model.

The covariance determination methodology was able to estimate the parameters of the input model, obtaining an RMS of the residuals between both parametric curves below a 2.2% of the maximum atmospheric density standard deviation. The estimated atmopsheric density model is close to the chosen theoretical model except at high altitudes, due to a deviation in the input perturbations caused by a limited amount of samples. Nonetheless, the covariance determination method has showed a satisfactory ability to estimate parameters affecting multiple objects of a catalog. Due to the properties of the Mahalanobis distance, the information of all objects could be treated as samples of the same distribution, allowing to determine properly the parameters of the density uncertainty. Due to departure from Gaussian assumption, the radial and cross-track components of the position differences were discarded from the computation of the Mahalanobis distance. However, the remaining in-track component is the direction where most of the density-related errors are expected to impact in the orbit, since the in-track direction is aligned with the velocity. The squared Mahalanobis distance distribution, after estimating the parameters of the uncertainty, presented a large similarity with the χ^2 distribution, confirmed by the Cramer-von-Mises statistic, which is an indicator of realism of the covariance. The averaged covariance containment results showed an improvement of the covariance realism in the catalog.

Regarding future work, a clear line of improvement is to analyse the sources of the non-Gaussianity in the radial and cross-track directions, to understand their origin and to be able to include them in the analysis. Moreover, the simulations must be extended to a larger amount of samples per altitude, in order to confirm the convergence of the methodology to the chosen atmospheric density model. Additionally, alternative state representations and covariance propagation techniques that are able to maintain Gaussianity for longer propagation arcs are to be investigated, such as in curvilinear coordinates or mean orbital elements. This is expected to provide better conditioned covariance matrices that improve the behaviour of the squared Mahalanobis distance distribution. It is also necessary to move towards more complex models for the dynamic model uncertainty, as opposed to the consider parameter theory with constant parameters. In this regard, time or space correlated noise models such as Ornstein-Uhlenbeck or Gauss-Markov processes are to be analysed, adapting the principles of the covariance determination method to the estimation of the parameters that define such stochastic models. Finally, further validation with real data is crucial to develop more flexible and complete methodologies to capture the uncertainty in real space environments.

REFERENCES

[1] B. D. Tapley, B. E. Schutz, and G. H. Born, *Statistical Orbit Determination*. San Diego, California: Elsevier Academic Press, 2004.

[2] D. A. Vallado, *Fundamentals of Astrodynamics and Applications*. Space Technology Library, Hawthorne, CA: Springer and Microcosm Press, forth ed., 1997.

[3] K. Alfriend and M. Wilkins, "Covariance as an estimator of orbit prediction error growth in the presence of unknown sensor biases," *American Astronomical Society*, vol. 103, pp. 99–422, 01 2000.

[4] O. Montenbruck and E. Gill, *Satellite Orbits: Models, Methods and Applications*. Berlin: Springer-Verlag Berlin Heidelberg, 2000.

[5] A. B. Poore, J. M. Aristoff, J. T. Horwood, R. Armellin, W. T. Cerven, Y. Cheng, C. M. Cox, R. S. Erwin, J. H. Frisbee, M. D. Hejduk, B. A. Jones, P. Di Lizia, D. J. Scheeres, D. A. Vallado, and R. M. Weisman, "Covariance and Uncertainty Realism in Space Surveillance and Tracking," tech. rep., Numerica Corporation Fort Collins United States, June 2016.

[6] M. Wilkins and K. Alfriend, "Characterizing orbit uncertainty due to atmospheric uncertainty," in *Astrodynamics Specialist Conference*, American Institute of Aeronautics and Astronautics, aug 2000.
[7] L. Sagnieres and I. Sharf, "Uncertainty characterization of atmospheric density models for orbit prediction of space debris," in *Proceedings of the 7th European Conference on Space Debris*, (Darmstadt, Germany), ESA Space Debris Ofice, 2017.
[8] M. Duncan and A. Long, "Realistic covariance prediction for the earth science constellation," in *AIAA/AAS Astrodynamics Specialist Conference and Exhibit*, American Institute of Aeronautics and Astronautics, aug 2006.
[9] M. Schubert, C. Kebschull, and S. Horstmann, "Analysis of different process noise models in typical orbitdetermination scenarios," in *8th European Conference on Space Debris*, vol. 8, (Darmstadt, German), ESA Space Debris Office, 2021.
[10] F. Schiemenz, J. Utzmann, and H. Kayal, "Least squares orbit estimation including atmospheric density uncertainty consideration," *Advances in Space Research*, vol. 63, pp. 3916–3935, jun 2019.
[11] J. H. Frisbee, "An empirical state error covariance matrix for weighted least squares estimation method," Tech. Rep. JSC-CN-24133, NASA Johnson Space Center Houston, TX, United States, January 2011.
[12] W. T. Cerven, "Covariance error assessment, correction, and impact on probability of collision," in *AAS/AIAA Space Flight Mechanics Meeting*, 2011.
[13] W. Cerven, "Improved empirical covariance estimation," *Advances in the Astronautical Sciences*, vol. 150, pp. 879–895, 01 2014.
[14] R. Zanetti and C. D'Souza, "Recursive implementations of the schmidt-kalman 'consider' filter," *The Journal of the Astronautical Sciences*, vol. 60, pp. 672–685, 2013.
[15] A. Jazwinski, *Stochastic processes and filtering theory*, vol. 64 of *Mathematics in science and engineering*. New York: Academic Press, Jan. 1970.
[16] J. L. Junkins, M. R. Akella, and K. T. Alfriend, "Non-gaussian error propagation in orbital mechanics," *Journal of The Astronautical Sciences*, vol. 44, pp. 541–563, 1996.
[17] D. A. Vallado and S. Alfano, "Curvilinear coordinates for covariance and relative motion operations," in *AAS/AIAA Astrodynamics Specialist Conference*, 2011. AAS 11-464.
[18] S. Laurens, J. Dolado, G. Cavallaro, M. Jouisse, and P. Seimandi, "Towards the maintenance of Gaussianity on state vector uncertainty propagation," in *69th International Astronautical Congress*, oct 2018. id: IAC-18,A6,9,3,x42351.
[19] Z. Folcik, A. Lue, and J. Vatsky, "Reconciling covariances with reliable orbital uncertainty," in *Advanced Maui Optical and Space Surveillance Technologies Conference*, p. E34, Sept. 2011.
[20] S. Laurens, P. Seimandi, J. Couetdic, and J. Dolado, "Covariance matrix uncertainty analysis and correction," in *68th International Astronautical Congress*, 2017. id: IAC-17,A6,7,2,x37415.
[21] A. Cano, A. Pastor, D. Escobar, J. Míguez, and M. Sanjurjo-Rivo, "Covariance determination for improving uncertainty realism in orbit determination and propagation," *Advances in Space Research*, 2022.
[22] A. Cano, A. Pastor, S. Fernández, J. Míguez, M. Sanjurjo-Rivo, and D. Escobar, "Improving orbital uncertainty realismthrough covariance determination in geo," *Journal of the Astronautical Sciences*, 2022, (accepted for publication, JASS-D-22-00019).
[23] A. Cano, A. Pastor, and D. Escobar, "Covariance determination for improving uncertainty realism," in *8th European Conference on Space Debris*, ESA Space Debris Office, 2021.
[24] D. A. Vallado and T. Kelso, "Earth orientation parameter and space weather data for flight operations," in *Advances in the Astronautical Sciences*, vol. 148, 2013. AAS 13-373.
[25] International Reference Atmosphere COSPAR, "Models of the earth's upper atmosphere," tech. rep., Committee on Space research (COSPAR) International Reference Atmosphere, 2012.
[26] D. J. Gondelach and R. Linares, *Atmospheric Density Uncertainty Quantification for Satellite Conjunction Assessment*.
[27] J. Emmert, H. Warren, A. Segerman, J. Byers, and J. Picone, "Propagation of atmospheric density errors to satellite orbits," *Advances in Space Research*, vol. 59, pp. 147–165, jan 2017.
[28] F. A. Marcos, S. T. Lai, C. Y. Huang, C. S. Lin, J. M. Retterer, S. H. Delay, and E. Sutton, "Towards next level satellite drag modeling," in *AIAA Guidance, Navigation, and Control Conference*, 2010.
[29] J. M. Leonard, J. M. Forbes, and G. H. Born, "Impact of tidal density variability on orbital and reentry predictions," tech. rep., American Geophysical Union, 2012.
[30] J. B. Aguado, J. L. Santiago, A. L. Yela, P. M. Olmos, J. M. Arenas, D. M. Gonzalez, M. S. Rivo, M. V. Lopez, A. Cano, D. Escobar, E. V. Bonay, P. G. Padreny, B. B. Virgili, S. Lemmens, K. Merz, and J. Siminski.,

"Uncertainty propagation meeting space debris needs," in *8th European Conference on Space Debris*, 2021.
[31] A. Cano, P. Gago, A. Pastor, J. L. Santiago, M. Sanjurjo-Rivo, J. Míguez, and D. Escobar, "Atmospheric correlation impact in uncertainty propagation," in *3rdInternational Conference on Space Situational Awareness(ICSSA)*, no. AA-ICSSA-22-0007, ICSSA, apr 2022.
[32] J. R. Michael, "The stabilized probability plot," *Biometrika*, vol. 70, no. 1, pp. 11–17, 1983.
[33] P. Royston, "Graphical detection of non-normality by using michael's statistic," *Applied Statistics*, vol. 42, no. 1, p. 153, 1993.
[34] P. Mahalanobis, "On the generalised distance in statistics," in *Proceedings of the National Institute of Sciences of India*, vol. 2, pp. 49–55, 1936.
[35] K. Hill, C. Sabol, and K. T. Alfriend, "Comparison of covariance based track association approaches using simulated radar data," *The Journal of the Astronautical Sciences*, vol. 59, pp. 281–300, jun 2012.
[36] R. B. D'Agostino and M. A. Stephens, *Goodness-of-fit techniques*, vol. 68 of *STATISTICS: Texbooks and Monographs*. New York: MARCEL DEKKER, INC, 1986.
[37] T. Kelso, "Celestrack SATCAT," 2020. [Online; accessed 22-January-2020].
[38] P. J. Brockwell and R. A. Davis, *Introduction to Time Series and Forecasting*. Springer, 2016.
[39] 18th Space Control Squadron, "Space-track," 2020. [Online; accessed 12-February-2020].
[40] D. A. Vallado and J. H. Seago, "Covariance realism," in *AAS/AIAA Astrodynamics Specialist Conference*, 2009.
[41] W. Wiesel, *Modern Orbit Determination*. Beavercreek, OH: Aphelion Press, 2003.